

COB-2023-0655

A PROTOTYPE FOR MULTIDIRECTIONAL ENERGY HARVESTING USING PENDULUM STRUCTURES AND HYBRID TRANSDUCTION

Luã Guedes Costa

Marcelo A. Savi

Universidade Federal do Rio de Janeiro, COPPE – Department of Mechanical Engineering, Center for Nonlinear Mechanics, 21.941.972, Rio de Janeiro, P.O. Box 68.503, Brazil.

guedes@mecanica.coppe.ufrj.br, savi@mecanica.coppe.ufrj.br

Abstract. *The search for sustainable and renewable forms of energy supply has led to the development of new and creative ways to convert available environmental energy into useful electrical energy. In this regard, mechanical energy sources such as vibrations, wind, and ocean waves, are abundant and can be harnessed to power from small electronic devices to small urban centers. Electromagnetic converters, piezoelectric materials, triboelectric structures, and magnetostrictive materials can be cited as viable options for energy harvesting, each with its own set of advantages and disadvantages. Energy harvesting systems that combines multiple transducer mechanisms have emerged as a promising trend in recent literature, as it has the potential to enhance energy harvesting capacity. Additionally, to ensure maximum efficiency in real-world applications, it is important to be able to harvest energy from multiple directions. This feature can be achieved by means of pendulum structures that can diffuse energy between directions within the system. This study investigates the combination of hybrid transducers and multidirectionality by analyzing a prototype of a hybrid electromagnetic-piezoelectric multidirectional energy harvester. Numerical analysis of the prototype are performed offering valuable insights about this type of electromechanical system. Results reveal that the addition of pendulum structures associated with hybrid transduction schemes can enhance energy harvesting performance significantly.*

Keywords: *Multidirectional Energy Harvesting, Smart Materials, Nonlinear Dynamics, Pendulum Structures, Hybrid Electromechanical Systems.*

1. INTRODUCTION

The continuous evolution of semiconductor technology is enabling the reduction of power consumption in electronic systems (Zhu *et al.*, 2020). This trend has sparked a growing interest in the potential of environmental mechanical energy sources, such as vibrations, sound, wind, and sea waves, as a viable alternative to traditional batteries and small-to-medium-sized systems. These sources of mechanical energy offer an attractive solution to the challenge of sustainable energy, with the ability to power a wide range of devices, from small electronics to small urban centers (Toprak and Tigli, 2014).

In order to harness the available mechanical energy in the environment and effectively convert it into electrical energy, the implementation of transduction mechanisms is essential. Electromagnetic converters, triboelectric structures and piezoelectric materials can be enumerated as some existing strategies to achieve this goal. Electromagnetic harvesters rely on the principle of electromagnetic induction and are commonly used in robust applications, ranging from micro to large scale applications (Cepnik *et al.*, 2013). In contrast, triboelectric structures use friction between two materials, typically polymers, to create an electric potential between two surfaces, making them more compact and suitable for nano to micro-scale applications (Haroun *et al.*, 2022). Lastly, piezoelectric materials are a class of smart materials that can convert mechanical to electrical energy through the reversible process of direct piezoelectric effect, which produces a proportional charge as a result of the application of a mechanical stress. Piezoelectric transducers can be applied to harvest energy from micro to large-scale applications (Clementi *et al.*, 2022).

In terms of efficiency in real applications, the hybridization strategy of mechanical energy harvesters utilizing different types of transducers is a trend in literature. By combining different types of transducers, the hybridization approach can exploit the unique advantages of each transducer, resulting in a greater energy harvesting capacity. Depending on the combination of transducers, various applications can be realized. For instance, Chung *et al.* (2021) utilized a Kresling origami structure that combined a rotational triboelectric and piezoelectric/triboelectric nanoconverters in contact mode. This innovative approach allowed the structure to take advantage of the rotational movement, the generated strain and contact, resulting in a better energy harvesting performance. Similarly, Zhong *et al.* (2015) utilized both electromagnetic and triboelectric transducers to build a hybrid energy harvester based on rotation to scavenge biomechanical energy as a mobile power source. Other researchers have also reported the use of various hybrid devices showing improved performance through the utilization of different conversion strategies (Yang and Cao, 2019; Halim *et al.*, 2019; Gao *et al.*,

2020; Xiao *et al.*, 2022). By leveraging the benefits of multiple transducers, hybrid energy harvesters can pave the way for more efficient and practical energy harvesting solutions.

Many of the harvesters documented in the literature are resonators such as beams, plates and springs. However, their effectiveness in converting energy is limited to frequencies near their natural frequency when operating in linear regime. This limitation has prompted researchers to propose nonlinear modulations in these systems, which can increase their bandwidth of operation and enable them to effectively harvest energy from the environment in practical applications. Multistable systems induced by magnets and by post-buckled structures can be cited as one of the most common nonlinearity modulations found in the literature (De Paula *et al.*, 2015; Costa *et al.*, 2021). Compared to the linear systems, this class of harvester can increase the performance of the system by increasing the maximum output power and bandwidth of operation (Stanton *et al.*, 2009). Nonsmooth impact-driven modulations are also a common way to greatly enhance the bandwidth of operation, but at the cost of maximum output power (Ai *et al.*, 2019). Also, the mechanical wear caused by successive impacts can be a drawback of this kind of harvester. Adeodato *et al.* (2021) and Yuan *et al.* (2019) showed that the usage of nonlinear smart structures, as shape memory materials, can be a viable solution to control and tune the natural frequency of the harvester, increasing the bandwidth of operation of the system in different scenarios.

At last, another concept that has been exploited in the literature is the capacity of harvest energy effectively in multiple directions. It has been shown that the usage of pendulum structures to achieve multidirectionality is a interesting and effective solution (Wu *et al.*, 2018).

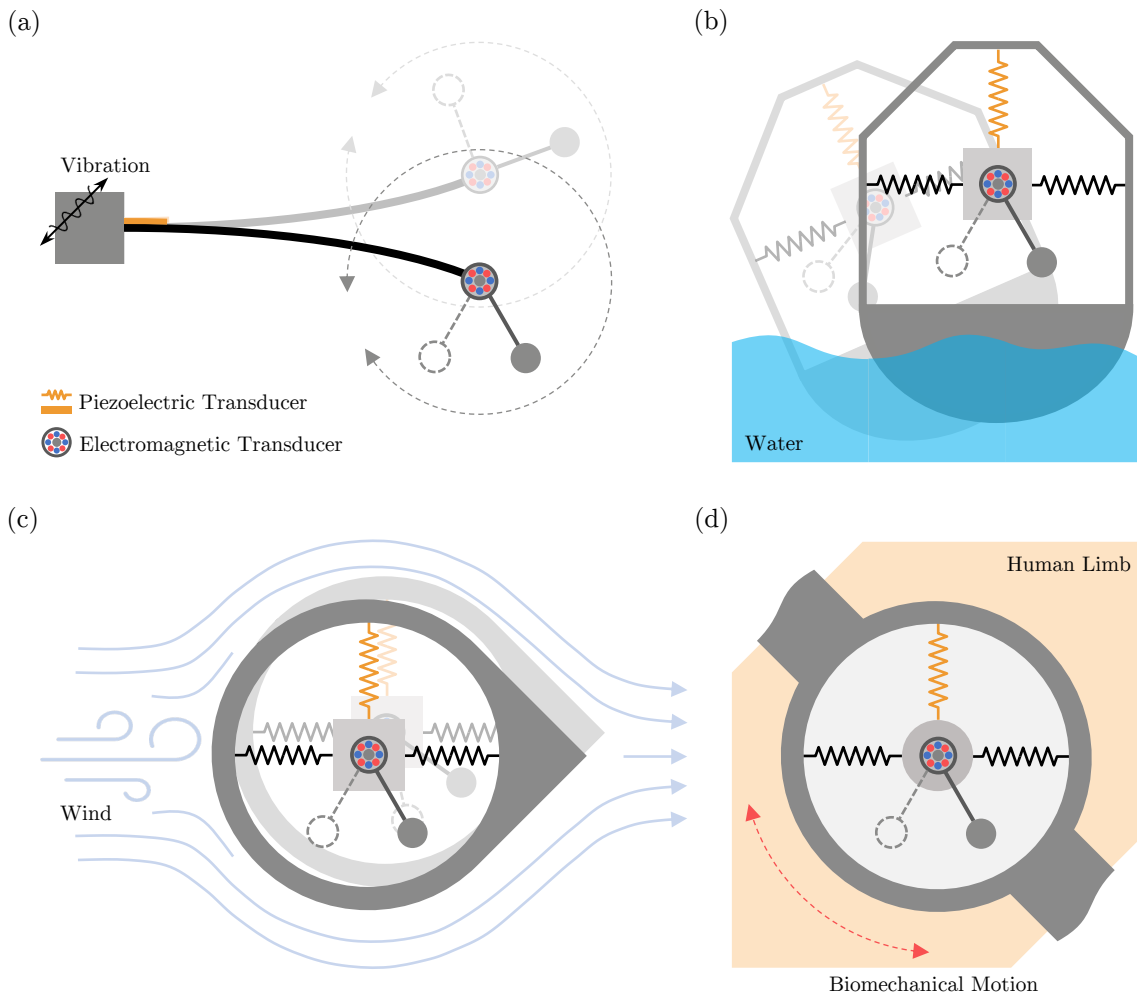


Figure 1: Examples of hybrid mechanical energy harvesters with an attached pendulum: (a) For vibration applications with a flexible cantilever beam as the main structure, (b) For offshore applications with a buoy as the base excitation structure, (c) For wind energy harvesting with a bluff body as the base excitation structure, (d) For biomechanical energy harvesting with a wearable device as the base excitation structure.

This work propose and analyzes an archetype reduced order model of a hybrid multidirectional pendulum energy harvester (HMEH), which focuses on capturing the main characteristics of this type of system. Specifically, a piezoelectric transducer is attached to the vertical direction of the harvester to convert energy from axial oscillations, while an electromagnetic converter is attached to the pendulum to harness the rotational energy.

2. ARCHETYPAL MODEL AND THEORETICAL BACKGROUND

Pendulum structures have been widely used in mechanical energy harvesting systems, as demonstrated in recent studies (Chen *et al.*, 2022; Wang, 2023). The aim of this work is to present a generic, reduced-order archetype model that captures the fundamental features of such systems and take advantage of the main characteristics of pendulum structures by adding an additional transducer to convert its rotational energy. Based on the ability to produce spring-type piezoelectric transducers (Kim *et al.*, 2015), Fig. 1 illustrates the concept of several systems that can be effectively represented by the proposed model. The applications range from vibration energy harvesting to offshore implementations, wind power conversion, and even biomechanical energy harvesting, underscoring the broad potential and versatility of the model.

2.1 Physical Modeling

Considering the examples displayed in Fig. 1, the hybrid multidirectional pendulum energy harvester (HMPEH) is represented by the archetype depicted in Fig. 2. The classical layouts of energy harvesters are designed to take advantage of incoming mechanical energy from only one direction in Cartesian space, making it potentially inefficient if the mechanical energy comes from a different direction. To overcome this problem, pendulum structures can be used to take advantage of its planar motion to transmit the input energy of one direction to another (for example: the energy flowing in the x axis transmitted to the z axis).

The modelling considers a generic main structure of effective mass m_s , and a pendulum-type element of effective mass m_p attached to it. The equivalent stiffness and damping coefficients are represented by k_i ($i = x, z, pz$) and c_j ($j = x, z, m, p$), in which subscripts are related to the direction or a element within the system. Subscript x and z refer to the plane directions, while subscript p refers to the pendulum, subscripts pz and m refers to the piezoelectric and electromagnetic transducers, respectively. These two transducers are attached to the system: a piezoelectric element with an electromechanical coupling term, θ_{pz} , and a equivalent stiffness, k_{pz} , in the z direction of the structure; and a electromagnetic energy converter attached to the pendulum with a electromagnetomechanical coupling term, θ_m , and a magnetic damping coefficient c_m . The transducers are represented by a equivalent circuit. The piezoelectric element can be represented by a circuit depicted in Fig. 2b, with a internal capacitance, C_{pz} , connected in parallel to an internal resistance R_{ipz} and a induced current related to the electromechanical coupling $I_{pz}(t) = \theta_{pz}\dot{z}_s(t)$. To the piezoelectric element is attached an external load resistance R_{lpz} . Additionally, the electromagnetic transducer is represented by the circuit depicted in Fig. 2c, with a voltage source, $v_m(t) = \theta_m\dot{\phi}(t)$, connected in series with an equivalent internal inductance, L_m , an internal resistance R_{iem} , and an external load resistance, R_{lem} . The equivalent resistance of the piezoelectric circuit is represented by $R_{pz} = R_{ipz}R_{lpz} / (R_{lpz} + R_{ipz})$, while the equivalent resistance of the electromagnetic circuit is represented by $R_{em} = R_{iem} + R_{lem}$. The effects of gravity, g , are considered and the system is subjected to a base excitation $\mathbf{r}_b(t) = r_b(t) [\sin(\mu)\hat{\mathbf{e}}_x + \cos(\mu)\hat{\mathbf{e}}_z]$, where μ is the angle between the external excitation vector $\mathbf{r}_b(t)$ and the z direction, and $r_b(t)$ is the excitation function.

The absolute structure position can be written as seen in Equation 1,

$$\begin{aligned} \mathbf{r}_s(t) &= [x_b(t) + x_s(t)]\hat{\mathbf{e}}_x + [z_b + z_s(t)]\hat{\mathbf{e}}_z \\ &= [x_b(t) + x(t)]\hat{\mathbf{e}}_x + [z_b(t) + z(t) + z_{st}]\hat{\mathbf{e}}_z \end{aligned} \quad (1)$$

where $x(t)$ and $z(t)$ are the relative positions in which the system oscillates in relation to the equilibrium position, and $z_{st} = (m_s + m_p)g / (k_z + k_{pz})$ is the static deflection of the structure due to gravity action. Also, the absolute position of the pendulum is determined by Equation 2.

$$\begin{aligned} \mathbf{r}_p(t) &= [x_b(t) + x(t) + x_p(t)]\hat{\mathbf{e}}_x + [z_b(t) + z(t) + z_{st} + z_p(t)]\hat{\mathbf{e}}_z \\ &= [x_b(t) + x(t) + L_p \sin(\phi(t))]\hat{\mathbf{e}}_x + [z_b(t) + z(t) + z_{st} + L_p \cos(\phi(t))]\hat{\mathbf{e}}_z \end{aligned} \quad (2)$$

Thus, the total kinetic energy can be written as the composition of the structure and the pendulum kinetic energies as described in Equation 3.

$$\begin{aligned} T &= T_s + T_p \\ &= \frac{1}{2}m_s\dot{\mathbf{r}}_s(t) \cdot \dot{\mathbf{r}}_s(t) + \frac{1}{2}m_p\dot{\mathbf{r}}_p(t) \cdot \dot{\mathbf{r}}_p(t) \\ &= \frac{1}{2}m_p \left\{ \left[\dot{x}(t) + \dot{x}_b(t) + L\dot{\phi}(t) \cos(\phi(t)) \right]^2 + \left[\dot{z}(t) + \dot{z}_b(t) - L\dot{\phi}(t) \sin(\phi(t)) \right]^2 \right\} \\ &\quad + \frac{1}{2}m_s \left\{ \left[\dot{x}(t) + \dot{x}_b(t) \right]^2 + \left[\dot{z}(t) + \dot{z}_b(t) \right]^2 \right\} \end{aligned} \quad (3)$$

The structure and piezoelectric element constitutive behaviors are assumed to be linear and, therefore, the total restitution forces of the structure springs, and the piezoelectric elements attached to the structure are defined in Equations 4,

5, and 6,

$$f_x(t) = -k_x x(t) \quad (4)$$

$$f_z(t) = -k_z z(t) \quad (5)$$

$$f_{pz}(t) = -k_{pz} z(t) \quad (6)$$

resulting in the total potential energy, written as the sum of the main structure, piezoelectric element and pendulum potential energies as depicted in Equation 7.

$$\begin{aligned} U &= U_s + U_p \\ &= - \int_0^{x_s(t)} f_x(t) dx - \int_0^{z_s(t)} [f_z(t) + f_{pz}(t)] dz - \int_0^{z_b(t)+z_s(t)} m_s g dz \\ &\quad - \int_0^{z_b(t)+z_s(t)+z_p(t)} m_p g dz \\ &= \frac{1}{2} k_x x(t)^2 + \frac{1}{2} (k_z + k_{pz}) [z(t) + z_{st}]^2 - m_s g [z_b(t) + z(t) + z_{st}] \\ &\quad - m_p g [z_b(t) + z(t) + z_{st} + L_p \cos(\phi(t))] \end{aligned} \quad (7)$$

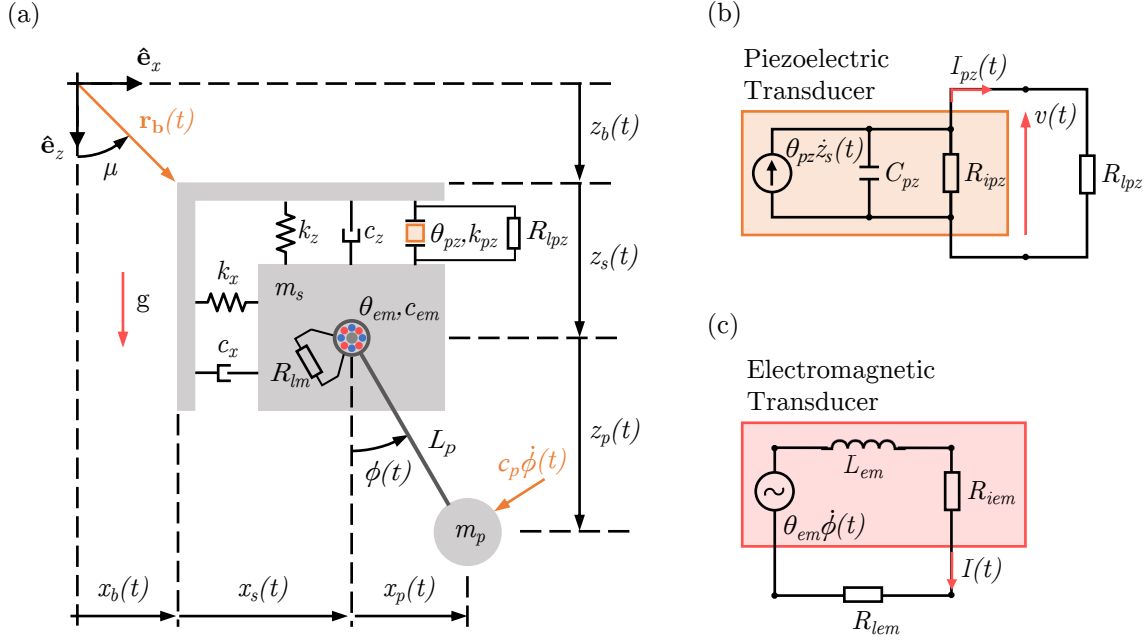


Figure 2: (a) Archetype representing the Hybrid Multidirectional Energy Harvester. (b) The equivalent circuit of the piezoelectric transducer attached to a resistance. (c) The equivalent circuit of the electromagnetic transducer attached to a resistance.

The electromechanical coupling of the piezoelectric transducer, θ_{pz} , is related to the induced current, $I_{pz}(t)$. In contrast, the magneto-electromechanical coupling of the electromagnetic transducer, θ_{em} , is related to the induced voltage, $v_{em}(t)$. The electromechanical coupling, θ_{pz} , is determined by the properties of the piezoelectric material, its geometry and dimensions. In contrast, the electromagnetomechanical coupling, θ_{em} , can be determined by the geometric characteristics of the coil(s), the properties of the magnet(s), the intensity of its magnetic field(s) and how these elements are positioned and distributed within the transducer. Often it is possible to determine these two quantities analytically, however for very complex structures finite element analysis or experimental methods are required. Another possibility is that these coupling mechanisms can dynamically change depending on the state of the system. In this work, to simplify matters, the coupling coefficients are considered constants.

From this perspective, consider the relation between the flux linkage, $\psi(t)$, and the voltage, $v(t)$, across the piezoelectric circuit as $\psi(t) = v(t)$, and the relation between the charge, $q(t)$, and the current, $I(t)$, flowing in the electromagnetic circuit as $\dot{q}(t) = I(t)$. Considering that, the total coenergy, W^* , of the system can be represented by the sum of the electric coenergy of the piezoelectric element, W_e^* , and the magnetic coenergy of the electromagnetic

transducer, W_m^* , as described by Equation 8, where W_C^* , W_{pz}^* , W_L^* and W_{em}^* are the electric coenergy in the capacitance, the piezoelectric coenergy, the magnetic coenergy in the inductance and the electromagnetic coenergy, respectively. The details of this formulation can be seen in (Preumont, 2006).

$$W^* = W_e^* + W_m^* \quad (8)$$

$$= W_C^* + W_{pz}^* + W_L^* + W_{em}^* \quad (9)$$

$$= \frac{1}{2}C_{pz}\dot{\psi}(t)^2 + \theta_{pz}\dot{\psi}(t)z(t) + \frac{1}{2}L_{em}\dot{q}(t)^2 + \theta_{em}\dot{q}(t)\phi(t) \quad (10)$$

The dissipation of the system is summarized in four major sources: viscous damping of the main structure; viscous damping of the pendulum structure; magnetic damping resulting from the interactions between magnet(s) and coil(s) within the electromagnetic transducer; and electrical resistances within circuits. These sources can be modeled through nonconservative virtual works acting on the system (Meirovitch, 2010), as depicted by Equation 11, where δW_{D_x} and δW_{D_z} are the virtual works done by the nonconservative forces in x and z directions, δW_{D_ϕ} is the total virtual work done by the moment of the nonconservative viscous force acting on the pendulum and the magnetic forces within the electromagnetic transducer, $\delta W_{R_{pz}}$ and $\delta W_{R_{em}}$ are the virtual works accounted for the resistive elements.

$$\begin{aligned} \delta W_{nc} &= \delta W_{D_x} + \delta W_{D_z} + \delta W_{D_\phi} + \delta W_{R_{pz}} + \delta W_{R_{em}} \\ &= -c_x\dot{x}(t)\delta x(t) - c_z\dot{z}(t)\delta z(t) - c_pL_p\dot{\phi}(t)\delta\phi(t) - c_{em}\dot{\phi}(t)\delta\phi(t) - \frac{\dot{\psi}(t)}{R_{em}}\delta\psi(t) \\ &\quad - R_{em}\dot{q}(t)\delta q(t) \end{aligned} \quad (11)$$

On this basis, by applying in the method of Euler-Lagrange for electromechanical systems (Equation 12) associated with five generalized coordinates, in which three are mechanical and two are electrical, $\mathbf{Q} = [x(t), z(t), \phi(t), \psi(t), q(t)]$,

$$\frac{d}{dt} \left(\frac{\partial \mathcal{L}}{\partial \dot{Q}_i} \right) - \frac{\partial \mathcal{L}}{\partial Q_i} = \frac{d\delta W_{nc}}{d\delta Q_i} \quad (12)$$

Suppressing the (t) in the notation of the generalized coordinates, the Euler-Lagrange electromechanical equations of the system can be written as a system of equations dependent of x , z , ϕ , v and I :

$$(m_s + m_p)\ddot{x} + c_x\dot{x} + k_x x + m_p L_p \left[\ddot{\phi} \cos(\phi) - \dot{\phi}^2 \sin(\phi) \right] = -(m_s + m_p)\ddot{x}_b \quad (13)$$

$$\begin{aligned} (m_s + m_p)\ddot{z} + c_z\dot{z} + (k_z + k_{pzt})z - \theta_{pz}v - m_p L_p \left[\ddot{\phi} \sin(\phi) + \dot{\phi}^2 \cos(\phi) \right] = \\ - (m_s + m_p)\ddot{z}_b \end{aligned} \quad (14)$$

$$\begin{aligned} m_p L_p^2 \ddot{\phi} + (c_{em} + c_p L_p)\dot{\phi} - \theta_{em}I + m_p L_p \left[\ddot{x} \cos(\phi) + g - \ddot{z} \right] \sin(\phi) = \\ m_p L_p \left[\ddot{z}_b \sin(\phi) - \ddot{x}_b \cos(\phi) \right] \end{aligned} \quad (15)$$

$$C_{pz}\dot{v} + \frac{v}{R_{pz}} + \theta_{pz}\dot{z} = 0 \quad (16)$$

$$L_{em}\dot{I} + R_{em}I + \theta_{em}\dot{\phi} = 0 \quad (17)$$

If the external forcing parameter is considered harmonic, then:

$$\mathbf{r}_b = x_b \hat{\mathbf{e}}_x + z_b \hat{\mathbf{e}}_z = A \sin(\omega t) \left[\sin(\mu) \hat{\mathbf{e}}_x + \cos(\mu) \hat{\mathbf{e}}_z \right] \quad (18)$$

Thus,

$$\ddot{\mathbf{r}}_b = \ddot{x}_b \hat{\mathbf{e}}_x + \ddot{z}_b \hat{\mathbf{e}}_z = -A\omega^2 \sin(\omega t) \left[\sin(\mu) \hat{\mathbf{e}}_x + \cos(\mu) \hat{\mathbf{e}}_z \right] \quad (19)$$

In order to generalize the analysis of the system, a normalization approach is performed by considering a reference length, L , a reference voltage V , and a reference current \mathcal{I} , resulting in the dimensionless electromechanical equations given by:

$$(1 + \rho)\ddot{\bar{x}} + 2\zeta_x\dot{\bar{x}} + \Omega_s^2\bar{x} + \rho\ell \left[\ddot{\bar{\phi}} \cos(\bar{\phi}) - \dot{\bar{\phi}}^2 \sin(\bar{\phi}) \right] = -(1 + \rho)\ddot{\bar{x}}_b \quad (20)$$

$$(1 + \rho)\ddot{\bar{z}} + 2\zeta_z\dot{\bar{z}} + \bar{z} - \chi_{pz}\bar{v} - \rho\ell \left[\ddot{\bar{\phi}} \sin(\bar{\phi}) + \dot{\bar{\phi}}^2 \cos(\bar{\phi}) \right] = -(1 + \rho)\ddot{\bar{z}}_b \quad (21)$$

$$\ddot{\bar{\phi}} + 2\zeta_\phi\dot{\bar{\phi}} + \Omega_\phi^2 \sin(\bar{\phi}) - \chi_{em}\bar{I} + \frac{1}{\ell} \left[\ddot{\bar{x}} \cos(\bar{\phi}) - \ddot{\bar{z}} \sin(\bar{\phi}) \right] = \frac{1}{\ell} \left[\ddot{\bar{z}}_b \sin(\bar{\phi}) - \ddot{\bar{x}}_b \cos(\bar{\phi}) \right] \quad (22)$$

$$\dot{\bar{v}} + \varphi_{pz}\bar{v} + \kappa_{pz}\dot{\bar{z}} = 0 \quad (23)$$

$$\dot{\bar{I}} + \varphi_{em}\bar{I} + \kappa_{em}\dot{\bar{\phi}} = 0 \quad (24)$$

that are related to the dimensionless parameters presented in Table 1.

Table 1: System parameters and values used in the analyses

Parameter Description	Symbol	Definition	Value
Linearized natural frequency of the main structure in x	ω_x	$\sqrt{k_x/m_s}$	-
Linearized natural frequency of the main structure in z	ω_z	$\sqrt{k_z/m_s}$	-
Linearized natural frequency of the pendulum	ω_ϕ	$\sqrt{g/L_p}$	-
Normalized time	τ	$\omega_z t$	-
Normalized x displacement of the main structure	$\bar{x}(\tau)$	$x(t)/L$	-
Normalized z displacement of the main structure	$\bar{z}(\tau)$	$z(t)/L$	-
Normalized angle of the pendulum structure	$\bar{\phi}(\tau)$	$\phi(t)$	-
Normalized voltage of the piezoelectric circuit	$\bar{v}(\tau)$	$v(t)/V$	-
Normalized current of the electromagnetic circuit	$\bar{I}(\tau)$	$I(t)/\mathcal{I}$	-
Normalized base excitation frequency	Ω	ω/ω_z	0.01 \rightarrow 2
Normalized base excitation amplitude	γ	A/L	0.01 \rightarrow 1
Normalized angle of the base excitation vector $\mathbf{r}_b(t)$	$\bar{\mu}$	μ	0°, 45°, 90°
Normalized base excitation displacement in the x direction	$\bar{x}_b(\tau)$	$\gamma \sin(\Omega\tau) \sin(\bar{\mu})$	-
Normalized base excitation displacement in the z direction	$\bar{z}_b(\tau)$	$\gamma \sin(\Omega\tau) \cos(\bar{\mu})$	-
Ratio of masses	ρ	m_p/m_s	0.5
Normalized damping coefficient of the main structure in x	ζ_x	$c_x/(2\omega_x m_s)$	0.025
Normalized damping coefficient of the main structure in z	ζ_z	$c_z/(2\omega_z m_s)$	0.025
Normalized total damping coefficient of the pendulum structure	ζ_ϕ	$\frac{[(c_{em}/L_p) + c_p]}{2\omega_z L_p m_s}$	0.0025
Ratio of natural frequencies of the main structure	Ω_s	ω_x/ω_z	0.01 \rightarrow 2.0
Ratio of natural frequencies of the pendulum and the z direction	Ω_ϕ	ω_ϕ/ω_z	0.01 \rightarrow 2.0
Normalized pendulum length	ℓ	L_p/L	1
Normalized piezoelectric coupling in the mechanical ODE	χ_{pz}	$\theta_{pz} V / (k_z L)$	0.05
Normalized magnetomechanical coupling in the mechanical ODE	χ_{em}	$\theta_{em} \mathcal{I} / (\rho k_z L_p^2)$	0.01
Normalized piezoelectric coupling in the piezo circuit ODE	κ_{pz}	$\theta_{pz} L / (C_{pz} V)$	0.5
Normalized EM coupling in the electromagnetic circuit ODE	κ_{em}	$\theta_{em} / (L_{em} \mathcal{I})$	0.1
Normalized equivalent resistance of the piezoelectric circuit	φ_{pz}	$1 / (C_{pz} R_{pz} \omega_z)$	0.05
Normalized equivalent resistance of the electromagnetic circuit	φ_{em}	$R_{em} / (L_{em} \omega_z)$	0.05
Normalized electrical output power of the piezoelectric circuit	$\bar{P}_{pz}(\tau)$	$P_{pz}(t) / (C_{pz} \omega_z V^2)$	-
Normalized electrical output power of the electromagnetic circuit	$\bar{P}_{em}(\tau)$	$P_{em}(t) / (L_{em} \omega_z \mathcal{I}^2)$	-

2.2 Performance Metrics

The performance of the energy harvesting system is evaluated with the definition of the electrical power dissipated by both piezoelectric and electromagnetic circuits. The total instantaneous electrical power consists by the sum of the instantaneous electrical power in each circuit, as represented by Equation 25. Thus, the average electrical power, defined over the interval $t_0 \leq t \leq t_f$, is represented by Equation 26, where v^{RMS} and I^{RMS} are the root mean square of the output voltage of the piezoelectric circuit and the output current of the electromagnetic circuit, respectively, and is defined as depicted in Equation 27.

$$P = P_{pz} + P_{em} = \frac{1}{R_{pz}} v^2 + R_{em} I^2 \quad (25)$$

$$P_{\text{avg}} = \frac{1}{t_f - t_0} \int_{t_0}^{t_f} P dt = \frac{1}{R_{pz}} (v^{\text{RMS}})^2 + R_{em} (I^{\text{RMS}})^2 \quad (26)$$

$$g_i^{\text{RMS}} = \sqrt{\frac{1}{t_f - t_0} \int_{t_0}^{t_f} g_i(t)^2 dt}, \quad \mathbf{g}(t) = \{v(t), I(t)\} \quad (27)$$

Furthermore, based on these concepts and according to Table 1, the normalized average electrical output power can be determined as described in Equation 28.

$$\bar{P}_{\text{avg}} = \bar{P}_{pz} + \bar{P}_{em} = \varphi_{pz} (\bar{v}^{\text{RMS}})^2 + \varphi_{em} (\bar{I}^{\text{RMS}})^2 \quad (28)$$

3. ACHIEVING EFFICIENT MULTIDIRECTIONALITY USING A PENDULUM STRUCTURE

Realistically, in any application, mechanical input sources occur usually in more than one direction. Many designs of harvesters only consider 1 direction of operation, limiting the harvester's efficiency. To illustrate that, consider the archetypes presented in Fig. 3, where 3 cases are established: Case I refers to the system without the pendulum, that is, maintaining the pendulum's mass and reducing ℓ to zero. This configuration can be achieved by making $\zeta_\phi = \Omega_\phi = \ell = \chi_{em} = \kappa_{em} = \varphi_{em} = 0$. Case II refers to the system with the pendulum structure, but without the electromagnetic converter. This configuration can be achieved by making $\chi_{em} = \kappa_{em} = \varphi_{em} = 0$. Finally, case III refers to the proposed system, with the pendulum structure and the electromagnetic converter. Non-zero parameters are utilized as presented in Table 1.

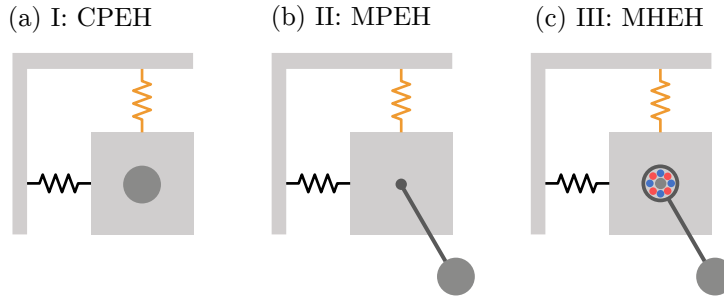


Figure 3: Simplified illustrations of (a) Case I: The classical linear piezoelectric energy harvester (CPEH). (b) Case II: The multidirectional piezoelectric energy harvester (MPEH), with the multidirectionality induced by the pendulum structure attached to the mass. (c) Case III: The multidirectional hybrid energy harvester (MHEH), proposed in this work. The hybridization is achieved by the simultaneous usage of a piezoelectric and a electromagnetic transducer.

The performance of each system is assessed across a range of frequencies by imposing various excitation angles for each case. \bar{P}_{avg} vs Ω diagrams, presented in Figs. 4, 5 and 6, are constructed by employing the fourth order Runge-Kutta scheme, considering a time step $\Delta\tau \propto 2\pi/\Omega$. $\bar{x} = \dot{\bar{x}}_0 = \bar{z}_0 = \dot{\bar{z}}_0 = \bar{\phi}_0 = \dot{\bar{\phi}}_0 = \bar{v}_0 = \dot{\bar{I}}_0 = 0$ are used as initial conditions. A progressive sweep in ascending order of the frequency, Ω , was performed. For each step, $\Delta\Omega$, 1000 excitation periods, T , are imposed at each integration, with the last 250 considered to be steady state. The value of the steady state average output power, \bar{P}_{avg} , is computed for each step. As Ω increases, the dynamics of the system was maintained, that is, besides for the first value of Ω , the initial conditions of each point in the diagram corresponded to the end state of the preceding point. Different excitation levels of $\gamma = 0.1$, $\gamma = 0.25$, and $\gamma = 0.5$ are considered.

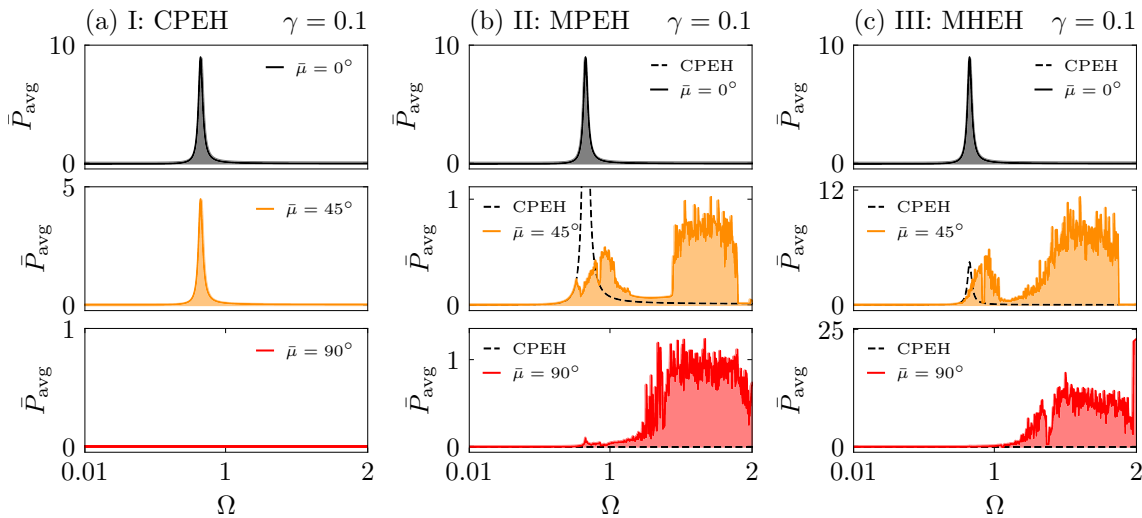


Figure 4: Cases represented in Fig. 3 excited with different angles $\bar{\mu}$ for a normalized excitation amplitude of $\gamma = 0.1$. (a) Classical linear piezoelectric energy harvester (CPEH). (b) A comparison between the CPEH (dashed black lines) and the multidirectional piezoelectric energy harvester (MPEH). (c) A comparison between the CPEH (dashed black lines) the proposed multidirectional hybrid energy harvester (MHEH). The values of \bar{P}_{avg} are scaled by $\times 10^{-3}$.

In each of the Figures, the first column (a) illustrates the performance of case I: CPEH. It is observed that when the excitation angle, $\bar{\mu}$, is set to 0° , the system achieves maximum performance as the direction of excitation aligns parallel to the \hat{e}_z axis. However, as the angle $\bar{\mu}$ increases, the maximum power output diminishes gradually until it reaches zero at $\bar{\mu} = 90^\circ$, when the excitation becomes perpendicular to the \hat{e}_z axis. Consequently, for excitation angles other than $\bar{\mu} = 0^\circ$ and $\bar{\mu} = 180^\circ$, the CPEH system experiences a loss of valuable energy from the environment.

To address the issue, a pendulum structure can be used to achieve multidirectionality (referred to as case II: MPEH) as shown by (Xu and Tang, 2015; Pan *et al.*, 2019, 2021). Figures 4(b), 5(b) and 6(b) display the performance for this kind of harvester. For an excitation angle of $\bar{\mu} = 0^\circ$, the performance of the MPEH is identical to that of the CPEH as there is no resulting motion from the pendulum. In contrast, for an excitation angle of $\bar{\mu} = 90^\circ$ the advantages of utilizing a pendulum structure to facilitate energy transfer between directions become evident. In this scenario, the system is capable of effectively harvesting energy from all directions. However, for intermediate angles between $0^\circ < \bar{\mu} < 90^\circ$ the system exhibits a drawback: it demonstrates lower efficiency compared to the CPEH in certain scenarios. This is due to the

pendulum acting as an energy absorber.

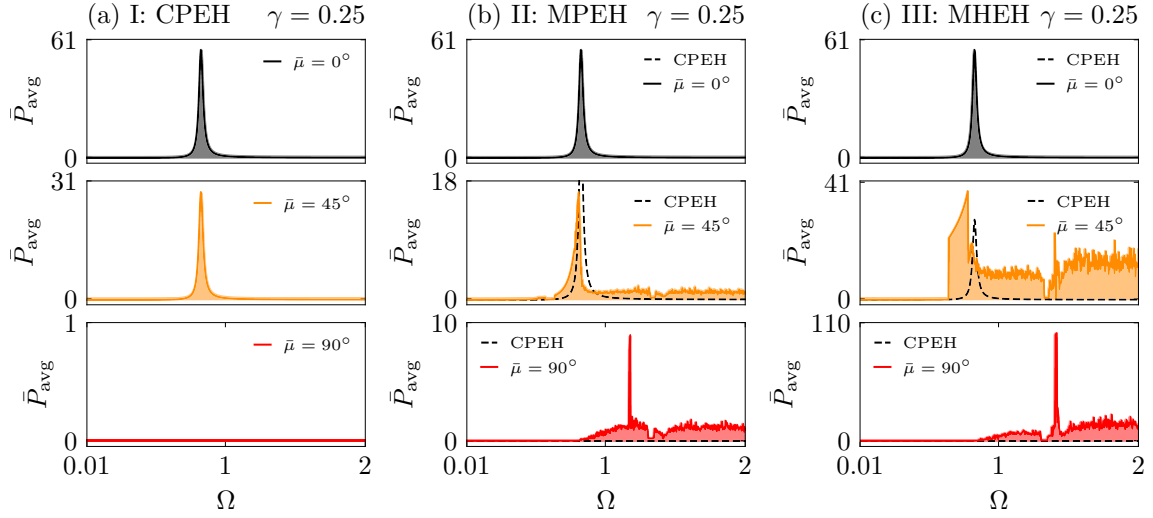


Figure 5: Cases represented in Fig. 3 excited with different angles $\bar{\mu}$ for a normalized excitation amplitude of $\gamma = 0.25$. (a) Classical linear piezoelectric energy harvester (CPEH). (b) A comparison between the CPEH (dashed black lines) and the multidirectional piezoelectric energy harvester (MPEH). (c) A comparison between the CPEH (dashed black lines) the proposed multidirectional hybrid energy harvester (MHEH). The values of \bar{P}_{avg} are scaled by $\times 10^{-3}$.

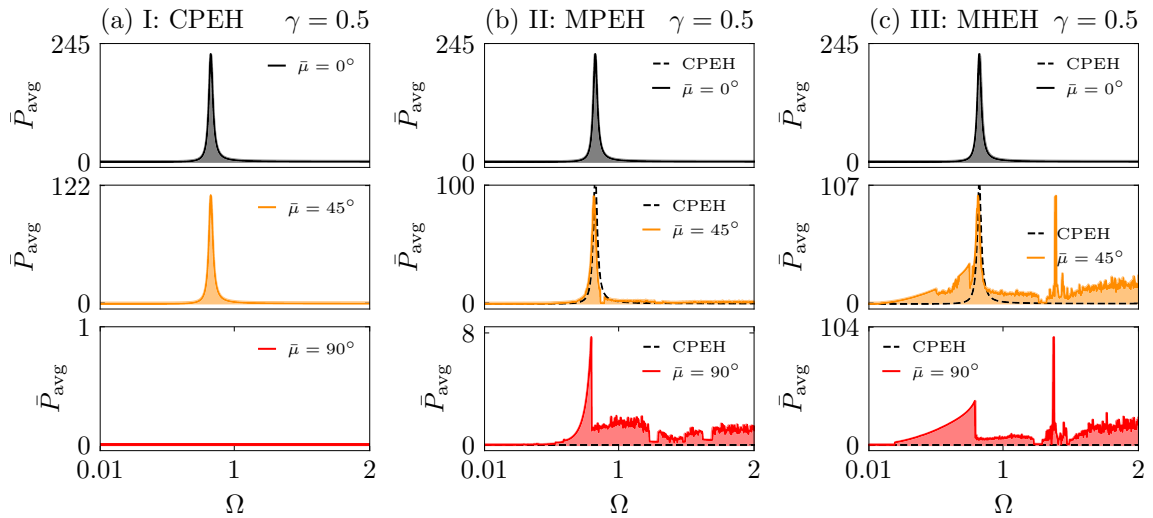


Figure 6: Cases represented in Fig. 3 excited with different angles $\bar{\mu}$ for a normalized excitation amplitude of $\gamma = 0.5$. (a) Classical linear piezoelectric energy harvester (CPEH). (b) A comparison between the CPEH (dashed black lines) and the multidirectional piezoelectric energy harvester (MPEH). (c) A comparison between the CPEH (dashed black lines) the proposed multidirectional hybrid energy harvester (MHEH). The values of \bar{P}_{avg} are scaled by $\times 10^{-3}$.

To deal with this matter, an electromagnetic transducer has been integrated into the system to harness the rotational energy, enabling some of the mechanical energy absorbed by the pendulum to be converted into electrical energy. This results into the hybrid system represented by the case III: MHEH. The performance of this harvester is presented in Figures 4(c), 5(c) and 6(c). Similar to the previous case, for an angle of $\bar{\mu} = 0^\circ$, the performance of the MHEH equivalent to the CPEH as there is no resulting motion of the pendulum. However, for angles of $\bar{\mu} = 45^\circ$ and $\bar{\mu} = 90^\circ$, there is an impressive increase of performance in both maximum output power and bandwidth when compared to the CPEH. These results establish the MHEH as a harvester that retains the desirable characteristics of the MPEH while mitigating its drawbacks.

4. CONCLUSIONS

This delves with the analysis of a proposed archetype generic reduced-order model designed to describe the fundamental characteristics of hybrid electromagnetic-piezoelectric multidirectional energy harvesting systems. These systems utilize pendulum structures to achieve multidirectionality and have potential applications in vibration, wave, wind, and biomechanical energy harvesting.

The archetype model serves as the foundation for this research. The performance metric employed is the average output electrical power, and three distinct cases are considered: (1) the classical piezoelectric energy harvester, which captures energy in a single direction; (2) the multidirectional piezoelectric energy harvester, comprising the same structure combined with a pendulum; and (3) the hybrid multidirectional energy harvester, which incorporates the piezoelectric energy harvester structure, the attached pendulum, and an additional electromagnetic transducer associated with the pendulum.

The results demonstrate that relying solely on the pendulum to achieve multidirectionality is insufficient in terms of efficiency, as the pendulum acts as an energy absorber, thereby reducing the system's overall performance. Conversely, employing a hybrid scheme by integrating an electromagnetic transducer with the pendulum proves to be a viable solution. This hybrid approach harnesses the rotational energy of the pendulum, allowing some of the mechanical energy absorbed by the pendulum to be converted into electrical energy. Consequently, the performance of these types of energy harvesters is significantly enhanced.

Overall, this study establishes the hybrid multidirectional energy harvester as a solution that maintains the desirable multidirectional characteristics while mitigating the drawbacks associated with attaching a pendulum without an associated harvester.

5. ACKNOWLEDGEMENTS

The authors would like to acknowledge the support of the Brazilian Research Agencies CNPq, CAPES and FAPERJ.

6. REFERENCES

- Adeodato, A., Duarte, B.T., Monteiro, L.L.S., Pacheco, P.M.C. and Savi, M.A., 2021. "Synergistic use of piezoelectric and shape memory alloy elements for vibration-based energy harvesting". *International Journal of Mechanical Sciences*, Vol. 194, p. 106206. ISSN 0020-7403. doi:10.1016/j.ijmecsci.2020.106206. URL <https://www.sciencedirect.com/science/article/pii/S0020740320343113>.
- Ai, R., Monteiro, L.L.S., Monteiro, P.C.C., Pacheco, P.M.C.L. and Savi, M.A., 2019. "Piezoelectric vibration-based energy harvesting enhancement exploiting nonsmoothness". *Actuators*, Vol. 8, No. 1. ISSN 2076-0825. doi:10.3390/act8010025. URL <https://www.mdpi.com/2076-0825/8/1/25>.
- Cepnik, C., Lausecker, R. and Wallrabe, U., 2013. "Review on electrodynamic energy harvesters—a classification approach". *Micromachines*, Vol. 4, No. 2, pp. 168–196. ISSN 2072-666X. doi:10.3390/mi4020168. URL <https://www.mdpi.com/2072-666X/4/2/168>.
- Chen, J., Bao, B., Liu, J., Wu, Y. and Wang, Q., 2022. "Pendulum energy harvesters: A review". *Energies*, Vol. 15, No. 22. ISSN 1996-1073. doi:10.3390/en15228674. URL <https://www.mdpi.com/1996-1073/15/22/8674>.
- Chung, J., Song, M., Chung, S.H., Choi, W., Lee, S., Lin, Z.H., Hong, J. and Lee, S., 2021. "Triangulated cylinder origami-based piezoelectric/triboelectric hybrid generator to harvest coupled axial and rotational motion". *Research*, Vol. 2021. doi:10.34133/2021/7248579. URL <https://spj.science.org/doi/abs/10.34133/2021/7248579>.
- Clementi, G., Cottone, F., Di Michele, A., Gammaitoni, L., Mattarelli, M., Perna, G., López-Suárez, M., Baglio, S., Trigona, C. and Neri, I., 2022. "Review on innovative piezoelectric materials for mechanical energy harvesting". *Energies*, Vol. 15, No. 17. ISSN 1996-1073. doi:10.3390/en15176227. URL <https://www.mdpi.com/1996-1073/15/17/6227>.
- Costa, L.G., da Silva Monteiro, L.L., Pacheco, P.M.C.L. and Savi, M.A., 2021. "A parametric analysis of the nonlinear dynamics of bistable vibration-based piezoelectric energy harvesters". *Journal of Intelligent Material Systems and Structures*, Vol. 32, No. 7, pp. 699–723. doi:10.1177/1045389X20963188. URL <https://doi.org/10.1177/1045389X20963188>.
- De Paula, A.S., Inman, D.J. and Savi, M.A., 2015. "Energy harvesting in a nonlinear piezomagnetoelastic beam subjected to random excitation". *Mechanical Systems and Signal Processing*, Vol. 54-55, pp. 405–416. ISSN 0888-3270. doi:10.1016/j.ymsp.2014.08.020. URL <https://www.sciencedirect.com/science/article/pii/S0888327014003379>.
- Gao, L., Lu, S., Xie, W., Chen, X., Wu, L., Wang, T., Wang, A., Yue, C., Tong, D., Lei, W., Yu, H., He, X., Mu, X., Wang, Z.L. and Yang, Y., 2020. "A self-powered and self-functional tracking system based on triboelectric-electromagnetic hybridized blue energy harvesting module". *Nano Energy*, Vol. 72, p. 104684. ISSN 2211-2855. doi:10.1016/j.nanoen.2020.104684. URL

- <https://www.sciencedirect.com/science/article/pii/S221128552030241X>.
- Halim, M.A., Kabir, M.H., Cho, H. and Park, J.Y., 2019. "A frequency up-converted hybrid energy harvester using transverse impact-driven piezoelectric bimorph for human-limb motion". *Micromachines*, Vol. 10, No. 10. ISSN 2072-666X. doi:10.3390/mi10100701. URL <https://www.mdpi.com/2072-666X/10/10/701>.
- Haroun, A., Tarek, M., Mosleh, M. and Ismail, F., 2022. "Recent progress on triboelectric nanogenerators for vibration energy harvesting and vibration sensing". *Nanomaterials*, Vol. 12, No. 17. ISSN 2079-4991. doi:10.3390/nano12172960. URL <https://www.mdpi.com/2079-4991/12/17/2960>.
- Kim, D., Roh, H.S., Kim, Y., No, K. and Hong, S., 2015. "Selective current collecting design for spring-type energy harvesters". *RSC Adv.*, Vol. 5, pp. 10662–10666. doi:10.1039/C4RA16443A. URL <http://dx.doi.org/10.1039/C4RA16443A>.
- Meirovitch, L., 2010. *Methods of Analytical Dynamics*. Advanced engineering series. Dover Publications. ISBN 9780486432397.
- Pan, J.N., Qin, W.Y., Deng, W.Z. and Zhou, H.L., 2019. "Harvesting base vibration energy by a piezoelectric inverted beam with pendulum*". *Chinese Physics B*, Vol. 28, No. 1, p. 017701. doi:10.1088/1674-1056/28/1/017701. URL <https://dx.doi.org/10.1088/1674-1056/28/1/017701>.
- Pan, J., Qin, W., Deng, W., Zhang, P. and Zhou, Z., 2021. "Harvesting weak vibration energy by integrating piezoelectric inverted beam and pendulum". *Energy*, Vol. 227, p. 120374. ISSN 0360-5442. doi:10.1016/j.energy.2021.120374. URL <https://www.sciencedirect.com/science/article/pii/S036054422100623X>.
- Preumont, A., 2006. *Mechatronics: Dynamics of Electromechanical and Piezoelectric Systems*. Springer Netherlands, Dordrecht. ISBN 978-1-4020-4696-4. doi:10.1007/1-4020-4696-0.
- Stanton, S.C., McGehee, C.C. and Mann, B.P., 2009. "Reversible hysteresis for broadband magnetopiezoelectric energy harvesting". *Applied Physics Letters*, Vol. 95, No. 17, p. 174103. doi:10.1063/1.3253710. URL <https://doi.org/10.1063/1.3253710>.
- Toprak, A. and Tigli, O., 2014. "Piezoelectric energy harvesting: State-of-the-art and challenges". *Applied Physics Reviews*, Vol. 1, No. 3, p. 031104. doi:10.1063/1.4896166. URL <https://doi.org/10.1063/1.4896166>.
- Wang, T., 2023. "Pendulum-based vibration energy harvesting: Mechanisms, transducer integration, and applications". *Energy Conversion and Management*, Vol. 276, p. 116469. ISSN 0196-8904. doi:10.1016/j.enconman.2022.116469. URL <https://www.sciencedirect.com/science/article/pii/S019689042201247X>.
- Wu, Y., Qiu, J., Zhou, S., Ji, H., Chen, Y. and Li, S., 2018. "A piezoelectric spring pendulum oscillator used for multi-directional and ultra-low frequency vibration energy harvesting". *Applied Energy*, Vol. 231, pp. 600–614. ISSN 0306-2619. doi:10.1016/j.apenergy.2018.09.082. URL <https://www.sciencedirect.com/science/article/pii/S030626191831393X>.
- Xiao, Y., Niu, M., Yang, L., Liu, J., Lv, X. and Yang, P., 2022. "Integrated triboelectric-electromagnetic-piezoelectric self-rebounding energy harvester for human energy harvesting". *Advanced Materials Technologies*, Vol. 7, No. 11, p. 2200340. doi:10.1002/admt.202200340. URL <https://onlinelibrary.wiley.com/doi/abs/10.1002/admt.202200340>.
- Xu, J. and Tang, J., 2015. "Multi-directional energy harvesting by piezoelectric cantilever-pendulum with internal resonance". *Applied Physics Letters*, Vol. 107, No. 21. ISSN 0003-6951. doi:10.1063/1.4936607. URL <https://doi.org/10.1063/1.4936607>. 213902.
- Yang, T. and Cao, Q., 2019. "Dynamics and performance evaluation of a novel tristable hybrid energy harvester for ultra-low level vibration resources". *International Journal of Mechanical Sciences*, Vol. 156, pp. 123–136. ISSN 0020-7403. doi:10.1016/j.ijmecsci.2019.03.034. URL <https://www.sciencedirect.com/science/article/pii/S0020740318339080>.
- Yuan, J.H., Yang, Y.Z. and Zhang, Y.H., 2019. "A piezoelectric energy harvester with light-activated shape memory polymers". *Ferroelectrics*, Vol. 550, No. 1, pp. 98–111. doi:10.1080/00150193.2019.1652500. URL <https://doi.org/10.1080/00150193.2019.1652500>.
- Zhong, X., Yang, Y., Wang, X. and Wang, Z.L., 2015. "Rotating-disk-based hybridized electromagnetic-triboelectric nanogenerator for scavenging biomechanical energy as a mobile power source". *Nano Energy*, Vol. 13, pp. 771–780. ISSN 2211-2855. doi:10.1016/j.nanoen.2015.03.012. URL <https://www.sciencedirect.com/science/article/pii/S2211285515001081>.
- Zhu, J., Liu, X., Shi, Q., He, T., Sun, Z., Guo, X., Liu, W., Sulaiman, O.B., Dong, B. and Lee, C., 2020. "Development trends and perspectives of future sensors and mems/nems". *Micromachines*, Vol. 11, No. 1. ISSN 2072-666X. doi:10.3390/mi11010007. URL <https://www.mdpi.com/2072-666X/11/1/7>.

7. RESPONSIBILITY NOTICE

The author(s) is (are) solely responsible for the printed material included in this paper.